

LCDiXRay: a user-friendly program for powder diffraction indexing of columnar liquid crystals

Nicolas Godbert,^{a*} Alessandra Crispini,^a Mauro Ghedini,^a Manuela Carini,^b Francesco Chiaravalloti^c and Andrea Ferrise^d

^aCentro di Eccellenza CEMIF.CAL, LASCAMM CR-INSTM della Calabria, Dipartimento di Chimica e Tecnologie Chimiche, Università della Calabria, 87036 Arcavacata di Rende (CS), Italy,

^bDipartimento di Ingegneria per l'Ambiente ed il Territorio e Ingegneria Chimica, Università della Calabria, 87036 Arcavacata di Rende (CS), Italy, ^cDipartimento di Fisica, Università della Calabria, 87036 Arcavacata di Rende (CS), Italy, and ^dDipartimento di Informatica, Modellistica, Elettronica e Sistemistica, Università della Calabria, 87036 Arcavacata di Rende (CS), Italy. Correspondence e-mail: nicolas.godbert@unical.it

The formulation of a standard computerized procedure for the indexing of powder X-ray diffraction (PXRD) patterns of columnar liquid crystals, with the determination of all structural information extracted from a properly indexed PXRD spectrum and the attribution of the columnar mesophase symmetry, is presented. In particular, the proposed program notably accelerates the identification of columnar mesophases together with the *in situ* determination of their structural parameters such as mesophase type, space group, cell parameters, cross-section area, intermolecular stacking distance between consecutive discoids and, in the case of ordered mesophases, the estimation of the number of molecules constituting each discoid.

© 2014 International Union of Crystallography

1. Introduction

Liquid crystals (LCs) are often characterized by powder X-ray diffraction (PXRD) analysis since the molecular organization within the mesophase gives rise to well defined PXRD patterns. Surprisingly, to the best of our knowledge, no specific computerized tools have been developed for the resolution of liquid crystal PXRD patterns. To date, the analysis of PXRD patterns has been performed manually by scientists through semi 'house-made' rules which are time consuming and often originate indexing mistakes, resulting in misleading determinations of the symmetries and/or cell parameters.

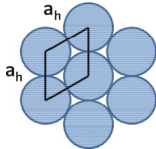
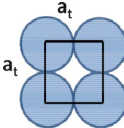
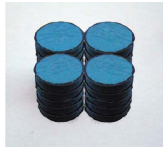
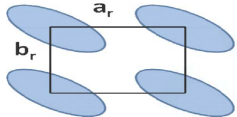
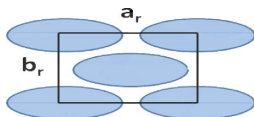
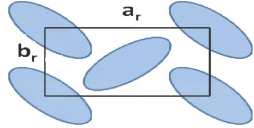
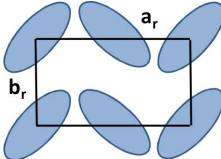
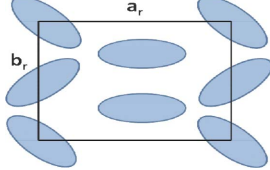
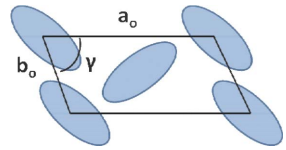
Columnar LCs (or discotics) can be divided according to their cell geometry into three different categories, columnar hexagonal (Col_h), columnar rectangular (Col_r) and columnar oblique (Col_o), which were first classified by Levelut in 1983 (Levelut, 1983). In addition, columnar tetrahedral structures (Col_t , also denoted Col_{sq}) have been observed for phthalocyanin liquid crystals, probably as a result of their peculiar structure (Ohta *et al.*, 1991; Komatsu *et al.*, 1994), and have been also encountered for nonconventional T-shaped polyphilic triblock molecules based on rod-like biphenyl core systems (Chen *et al.*, 2005). However, a Col_t phase can be considered as a Col_r mesophase of equal lattice parameters; in this regard, a detailed discussion will be presented below. Moreover, a columnar organization showing characteristics of both columnar and smectic phases is known as a lamello-columnar phase (Col_l). However, the indexing of PXRD patterns related to smectic mesophases will not be considered

in the present work. While discotics may also show low-ordered nematic mesophases [discotic nematic (N_D) and columnar nematic (N_C)], these LC phases will not be discussed in this report because of the lack of singularity of their PXRD patterns, due to the high intrinsic disorder. A comprehensive description of these mesophases is given in the excellent review written by Laschat *et al.* (2007), to which interested readers are referred. Moreover, highly ordered columnar mesophases presenting three-dimensional ordered structures such as H phase or plastic phases (Chandrasekhar *et al.*, 2002) will not be considered in this report.

The present article reports on standardized guidelines for the indexing of columnar liquid crystal PXRD patterns and the implementation of these guidelines in the program *LCDiXRay*. This protocol is based on necessary initial hypotheses coupled with mathematical expressions specific to each mesophase type. In this way the generation of various sets of possible indexing values is allowed. Comparing the obtained sets with experimental data, the identification of the most likely solution is achieved, reducing the probability of error. Furthermore, from the generated data set reproducing the experimental PXRD pattern, it is straightforward to access all the structural parameters of the mesophase, such as unit cell geometry and dimension, cross-section area, intermolecular stacking distances, and number of molecules within the discoid constituting the columns for ordered mesophases. All the classical columnar mesophases included in this report are summarized in Table 1 with related schemes and structural parameters.

Table 1

Two-dimensional space groups of columnar liquid crystals with corresponding cross-section area and number of discoids (disc or ellipsoid) Z_{disc} in a cross section.

Type (notation)	Space group	Extinction rules	Cross section			Three-dimensional representation
			Schema	Area	Discoid number	
Columnar hexagonal (Col_h)	$p6mm$	No conditions		$S_h = a_h^2 3^{1/2} / 2$	$Z_{\text{disc}} = 1$	
Columnar tetragonal (Col_t)	$p4mm$	No conditions		$S_t = a_t^2$	$Z_{\text{disc}} = 1$	
Columnar rectangular (Col_r)	$p2mm$	No conditions		$S_r = a_r b_r$	$Z_{\text{disc}} = 1$	
	$c2mm$	$hk: h + k = 2n,$ $h0: h = 2n,$ $0k: k = 2n$			$Z_{\text{disc}} = 2$	
	$p2gg$	$hk: \text{no conditions},$ $h0: h = 2n,$ $0k: k = 2n$			$Z_{\text{disc}} = 2$	
	$p2mg$	$hk: \text{no conditions},$ $h0: \text{no conditions},$ $0k: k = 2n$			$Z_{\text{disc}} = 2^\dagger$	
					$Z_{\text{disc}} = 4^\dagger$	
	Columnar oblique (Col_o)	$p1$	No conditions		$S_o = a_o b_o \sin \gamma$	$Z_{\text{disc}} = 2$

\dagger The two different schematic representations of $p2mg$ are reported (Levelut, 1983; Laschat *et al.*, 2007; Tschierske, 2007; Grolik *et al.*, 2012).

1.1. General definition and properties of columnar liquid crystals

Since their first identification by X-ray diffraction data in 1977 by Chandrasekhar *et al.* (1977), columnar (or discotic) liquid crystals have received much attention and have

attracted growing interest, especially in the past decade, for their applicative role in optoelectronic devices such as light emitting diodes, photovoltaic cells, field effect transistors, liquid crystal displays and photoconductors (Schmidt-Mende *et al.*, 2002; Hesse *et al.*, 2010; Zheng *et al.*, 2011; Shimizu *et al.*,

2007; Kaafarani, 2011; Sergeev *et al.*, 2007). The high interest shown towards both organic and inorganic columnar liquid crystals is testified by the high number of dedicated peer reviews, regarding their structure, properties and applications, published over the past few years (Laschat *et al.*, 2007; Kaafarani, 2011; Sergeev *et al.*, 2007; Kumar, 2006; Kato *et al.*, 2006; Tschierske, 2007). The typical disc-like structure of discotic molecules comprises a flat and rigid aromatic core surrounded by numerous long flexible alkyl chains. The columnar organization is directed by π - π stacking interactions of the aromatic cores of the disc-shaped molecules (discoidal or ellipsoidal). However, discoids can be obtained by self-assembly of several molecules, held together *via* secondary interactions such as π - π stacking or hydrogen-bonding networks. Rod-like molecules have been also reported to self-assemble into ellipsoidal discs, originally observed through association of three single molecules (Guillon *et al.*, 1987) and, as recently reported, association of 15–19 single molecules (Shimogaki *et al.*, 2011). The presence of secondary interactions often contributes to increasing the order and stability of the resulting mesophase, widening the temperature range of the columnar organization. In conventional discotics, this can be achieved, for instance, by both increasing the dimension of the aromatic core and introducing, within the alkyl chains, some chemical functions favouring hydrogen bonds (Kumar, 2006; Gehringer *et al.*, 2005).

The concept of order in discotics is often ambiguous. There is a difference between the intrinsic order of columnar mesophases (within/between columns) and induced order of

the bulk material obtained through alignment. Indeed, discotics can be macroscopically aligned (in a homogenous manner) in two different ways: (i) in a homeotropic manner (*i.e.* all column directors are placed orthogonally to the substrate plane) or (ii) in a planar orientation (*i.e.* all column directors are parallel to the substrate). Alignment, required depending on the application sought, can be achieved by appropriate techniques or by using suitable substrates (Li *et al.*, 2010). Aligned samples could be described as a highly ordered discotic mesophase. However, the terminology Col_{ho}, Col_{ro}, Col_{oo}, indicating ordered hexagonal, rectangular and oblique columnar phases, respectively, is not referred to such aligned mesophases but only used for intrinsic ordered phases, *i.e.* when the intracolumnar degree of order is high enough to observe in the PXRD pattern the reflection referred to as h_0 , due to the diffraction generated by stacking of discoids. In the case of ordered columnar phases generated by stacking of molecules within the discoids, supplementary reflections ($h_i, i > 0$) can be observed in the wide-angle region. The difference between an ordered and a disordered columnar phase is illustrated in Fig. 1, together with their corresponding expected PXRD patterns. Accordingly, Col_{hd}, Col_{rd} and Col_{od} are referred to as disordered hexagonal, rectangular and oblique columnar phases, respectively.

2. Indexing of a PXRD pattern of columnar liquid crystals

For practical reasons, all the diffraction angles (2θ) will be converted into the interplanar spacing distances through the Bragg law,

$$d_{h'k'l} = \frac{\lambda}{2 \sin \theta} \quad \text{with} \quad \begin{cases} h' = nh \\ k' = nk \\ l' = nl \end{cases} \quad (1)$$

where θ is the diffraction angle, λ is the wavelength of the monochromatic X-ray beam, h, k, l are the Miller indices of the associated reflection and n is an integer. Hereafter, all diffractions will be considered as their distance equivalents instead of their diffraction angles.

As clearly seen from the schematized PXRD pattern of a columnar LC presented in Fig. 2, two different angle regions can be defined: the small-angle area (from $2\theta \simeq 0$ to *ca* $2\theta = 12$ – 15°) and the high-angle area (for $2\theta > \text{ca } 12$ – 15°), the latter characterized by the broad halo generated by the slow motion of the flexible molten alkyl chains. The centre of this broad peak is conventionally referred to as the h_{ch} reflection halo.

Within the small-angle area, only reflection peaks relative to the intercolumnar d_{hk0} distances are observable. In the wide-angle region characterized by the broad halo h_{ch} , only intracolumnar d_{00l} reflection peaks (note $d_{001} = h_0$), if any, can be present, together with all possible reflection peaks due to intradiscoidal stacking (h_i). The indexing of a columnar PXRD pattern will be performed by comparison between the experimental distances d_{hk0} observed in the small-angle region of the spectrum and the calculated data sets of d_{hk0} distances obtained through initial assumptions and mathematical

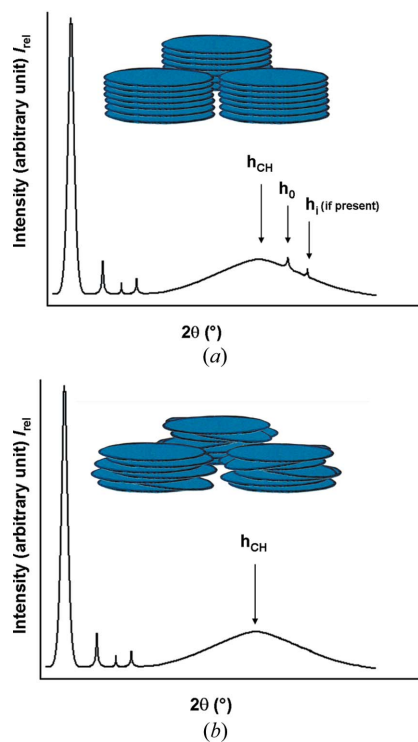


Figure 1 Ordered (a) and disordered (b) columnar phases and the schematic representation of their PXRD patterns. Note that for clarity all eventual d_{00l} peaks have been omitted.

expressions of the specific columnar mesophase relative to its two-dimensional lattice geometry. For columnar mesophases Col_h with hexagonal geometry,

$$\frac{1}{d_{hk0}^2} = \frac{4}{3} \left(\frac{h^2 + hk + k^2}{a_h^2} \right). \quad (2)$$

For columnar mesophases Col_r with rectangular geometry,

$$\frac{1}{d_{hk0}^2} = \frac{h^2}{a_r^2} + \frac{k^2}{b_r^2}. \quad (3)$$

For columnar mesophases Col_o with plane-parallel geometry

$$\frac{1}{d_{hk0}^2} = \frac{1}{\sin^2 \gamma} \left(\frac{h^2}{a_o^2} + \frac{k^2}{b_o^2} - \frac{2hk \cos \gamma}{a_o b_o} \right). \quad (4)$$

Here a_h , a_r and b_r , and a_o , b_o and γ are the cell parameters of the columnar hexagonal, rectangular and oblique mesophases, respectively (see Table 1 for cell drawings).

2.1. Indexing of the columnar hexagonal mesophase (Col_h)

As already reported in various studies (Laschat *et al.*, 2007; Chandrasekhar *et al.*, 2002), the indexing of a columnar hexagonal mesophase is rather straightforward, because of the high symmetry of the $p6mm$ space group. The calculation of a data set of interplanar spacing distances, as showed by equation (2), requires the determination of the unique unknown cell parameter a_h , implying the need of just one initial hypothesis. Taking into consideration the first reflection peak of the PXRD pattern ($d_{h_1k_10}$; Fig. 2) and assuming its identity as d_{100} , the following relations are easily deduced from equation (2):

$$\frac{1}{d_{100}^2} = \frac{4}{3a_h^2}, \quad a_h = \frac{2}{3^{1/2}} d_{100} \quad (5)$$

and

$$\frac{1}{d_{hk0}^2} = \frac{1}{d_{100}^2} (h^2 + hk + k^2). \quad (6)$$

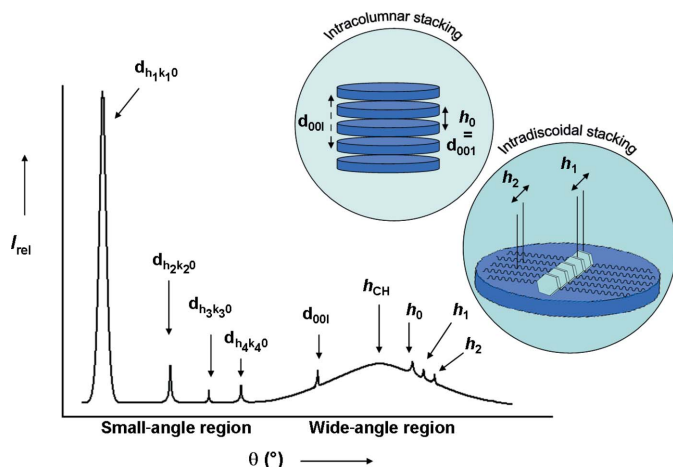


Figure 2
A general schematic PXRD pattern of a columnar liquid crystal. Note that several d_{00l} might be observed with $d_{00l} > d_{001}$.

Table 2

Characteristic ratios between the observed peaks of a PXRD pattern of a Col_h mesophase.

Peak	d_{100}	d_{110}	d_{200}	d_{210}	d_{300}	d_{220}	d_{310}	...	d_{hk0}	...
Ratio	1	$\frac{1}{3^{1/2}}$	$\frac{1}{2}$	$\frac{1}{7^{1/2}}$	$\frac{1}{3}$	$\frac{1}{12^{1/2}}$	$\frac{1}{13^{1/2}}$...	$\frac{1}{(h^2 + hk + k^2)^{1/2}}$...

Note: $d_{hkl} = d_{khl}$.

From the resulting equation (6), it is now evident that all interplanar spacing distances and therefore all the reflection peaks observed in the PXRD pattern will be in typical ratio values with respect to the first indexed peak. These ratio values calculated from equation (6) are reported in Table 2.

However, not all the d_{hk0} peaks will be necessarily observed, since the number and nature of the observed peaks depend highly on the intercolumnar degree of order. Note that the first observed peak $d_{h_1k_10}$, usually indexed as d_{100} , could be d_{110} or even of higher Miller indices in the case of very large diameter discoids. In this case, new correlation ratios between peaks have to be determined.

2.2. Indexing of columnar rectangular mesophases (Col_r)

The indexing of the PXRD pattern of a Col_r mesophase is more challenging because of the absence of a mathematical sequence as previously shown for the Col_h mesophase. Equation (3), which rules out interplanar spacing distances of a rectangular lattice geometry, clearly shows the dependency on two unknown unit-cell constants, a_r and b_r . Therefore, in the case of a Col_r PXRD pattern, an initial hypothesis for the first two reflection peaks of the spectrum ($d_{h_1k_10}$ and $d_{h_2k_20}$; Fig. 2), which are often observed rather close to each other, has to be imposed. The reason of the splitting of the first peak when passing from a Col_h to a Col_r mesophase has already been described (Laschat *et al.*, 2007; Chandrasekhar *et al.*, 2002). For each hypothetical value attributed to the couple h_1k_1/h_2k_2 used for indexing the first two peaks, a corresponding set of d_{hk0} values can be calculated and compared with the experimental d_{hk0} values. The calculation of these sets is based on the determination of the unknown constants A ($A = 1/a_r^2$) and B ($B = 1/b_r^2$) derived from equation (3), which can be rewritten for the chosen couple h_1k_1/h_2k_2 as

$$\frac{1}{d_{h_1k_10}^2} = Ah_1^2 + Bk_1^2, \quad (7)$$

$$\frac{1}{d_{h_2k_20}^2} = Ah_2^2 + Bk_2^2. \quad (8)$$

By combining these two equations, both A and B can be expressed and calculated as a function of the hypothesized first two reflection peaks.

Note that the most frequently encountered h_1k_1/h_2k_2 couples for Col_r mesophases are 11/20 and 20/11, but other combinations have also been reported, such as 11/02, 01/11, 11/31, 20/02 and 02/13 (Kilian *et al.*, 2000; Morale *et al.*, 2003; Pucci *et al.*, 2005; Venkatesan *et al.*, 2008; Maringa *et al.*, 2008;

Table 3

Characteristic ratios between the observed peaks of a PXRD pattern of a Col_t mesophase.

Peak	d_{100}	d_{110}	d_{200}	d_{210}	d_{220}	d_{300}	d_{310}	d_{230}	d_{140}	...	d_{hk0}	...
Ratio	1	$\frac{1}{2^{1/2}}$	$\frac{1}{2}$	$\frac{1}{5^{1/2}}$	$\frac{1}{8^{1/2}}$	$\frac{1}{3}$	$\frac{1}{10^{1/2}}$	$\frac{1}{13^{1/2}}$	$\frac{1}{17^{1/2}}$...	$\frac{1}{(h^2 + k^2)^{1/2}}$...

Note: $d_{hkl} = d_{khl}$.

Kaller *et al.*, 2009; Camerel *et al.*, 2006; Seo *et al.*, 2007; Wuckert *et al.*, 2009; Kaller *et al.*, 2010; Amaranatha Reddy *et al.*, 2005). Once the ideal calculated set has been identified, the unit-cell parameters can be easily extracted, being equal to d_{100} (a_r) and d_{010} (b_r), and the cross-section area can be calculated (see Table 1).

A direct comparison between the observed d_{hk0} distances of the PXRD pattern and the calculated sets generated through these equations gives rise to the best possible indexing of the studied spectrum.

The final analysis step to be performed is the eventual determination of the space group belonging to the studied Col_r mesophase. Four different space groups ($c2mm$, $p2mm$, $p2gg$ and $p2mg$) can be encountered and the accurate determination can be rather tricky. The space-group attribution is based on the presence and/or absence of reflection peaks, which implies the availability of a rather high number of reflections in the PXRD pattern, not so often occurring. Extinction rules relative to all lattice space groups and the corresponding illustrations are reported in Table 1.

2.3. Indexing of the columnar tetragonal mesophase (Col_t)

The Col_t mesophase can be considered as a Col_r mesophase with a unique cell parameter ($a_r = b_r$). Hence, equation (3) can be written as follows:

$$\frac{1}{d_{hk0}^2} = \frac{h^2 + k^2}{a_t^2}, \tag{9}$$

with a_t the lattice parameter of the Col_t mesophase (see Table 1).

As for the Col_h mesophase, adopting a similar analysis, the interplanar spacing distances are dependent on a sole unknown constant (a_t), and the resulting ratio values with respect to the first reflection, assumed to be d_{100} , can be extrapolated from equation (9); the results are collected in Table 3.

Again, not all reflections will be necessarily present in the PXRD pattern, though for the space group $p4mm$ of the tetragonal lattice, all reflections are theoretically allowed. Moreover, for very large discoids, the first observed peak $d_{h_1k_10}$ could differ from d_{100} , and hence new correlation ratios must be determined through equation (9). The Col_t mesophase is, however, less frequently encountered and often is observed in the case of highly specific shaped LCs (Ohta *et al.*, 1991; Komatsu *et al.*, 1994; Chen *et al.*, 2005).

2.4. Indexing of the columnar oblique mesophase (Col_o)

The columnar oblique mesophase (Col_o) represents the most complicated case in the indexing procedure. The presence of three consecutive rather close first reflection peaks in the small-angle region of the PXRD pattern is, however, the first indication of a possible Col_o mesophase. As clearly shown by equation (4), the introduction of the three unknown unit-cell parameters (a_o , b_o and γ) within the rather complex mathematical expression characterizes the Col_o lattice. Fortunately, the Col_o mesophase is more rarely encountered because strong core–core interactions between molecules are required to develop this phase (Laschat *et al.*, 2007). Similarly to the case of Col_r mesophases previously described, initial hypotheses for the resolution of the Col_o PXRD patterns have to be formulated. In this case, the indexing of the first three peaks of the spectrum ($d_{h_1k_10}$, $d_{h_2k_20}$ and $d_{h_3k_30}$; Fig. 2) has to be hypothesized. The calculation of the interplanar spacing distance sets will be performed through the determination of three unknown constants A [$A = 1/(a_o^2 \sin^2 \gamma)$], B [$B = 1/(b_o^2 \sin^2 \gamma)$] and C ($C = -2 \cos \gamma / a_o b_o \sin^2 \gamma$) derived from equation (4).

The PXRD pattern of a Col_o mesophase will be indexed by comparison between the experimental data and the sets of d_{hk0} values generated *via* the procedure summarized in the following scheme:

Col_o mesophase:

Sets of Interplanar spacing distances calculated by

$$\frac{1}{d_{hk0}^2} = Ah^2 + Bk^2 + Chk$$

with A, B and C determined taking in consideration the first three peaks of the PXRD pattern ($d_{h_1k_10}$, $d_{h_2k_20}$ and $d_{h_3k_30}$). The unit cell parameters are

$$\cos \gamma = \frac{d_{100}d_{010}}{4} \left(\frac{1}{d_{110}^2} - \frac{1}{d_{110}^2} \right), \quad a_o = d_{100} / \sin \gamma \quad \text{and} \quad b_o = d_{010} / \sin \gamma$$

Note that the symmetry of the Col_o lattice corresponds to the $p1$ space group, allowing all the $hk0$ reflections to be present. As already mentioned, Col_o mesophases are rarely observed and therefore it is difficult to define which initial triad values h_1k_1 , h_2k_2 , h_3k_3 are more frequently encountered for the indexing of the first three peaks. Examples reported for initial attribution are $20/11/1\bar{1}$, $10/11/2\bar{1}$, $11/20/1\bar{1}$ and $10/01/11$ (Morale *et al.*, 2003; Trzaska *et al.*, 1999; Choi *et al.*, 2011; Pucci *et al.*, 2011).

2.5. Indexing refinement

Once the most likely nature of the columnar mesophase has been identified, in order to obtain a data set of calculated d_{hk0} values with a more accurate fitting with respect to all the observed experimental ones, *i.e.* reducing the discrepancy between observed and calculated data, it is necessary to proceed to a re-evaluation (or refinement) of the values of the initial peaks, taking into account the maximum number of data available. Following this calculation, all the d_{hk0} peaks are

redetermined using the refined values, obviously through the mathematical expression of the identified mesophase.

For the Col_h mesophase, the value of d_{100} can be re-evaluated from equation (10) (Zelcer *et al.*, 2007):

$$d_{100}(\text{calcd}) = \frac{1}{N_{hk0}} \left[\sum_{hk0} d_{hk0}(\text{obs}) (h^2 + hk + k^2)^{1/2} \right], \quad (10)$$

where N_{hk0} is the number of $hk0$ observed reflections. For Col_l mesophases, the re-evaluation of the first two interplanar distances (d_{100} and d_{010}) can be performed. In order to take into account the maximum number of available data, it is recommended to determine first the mean value of d_{100} through equation (11) when the number of observed $h00$ reflections is higher than the number of $0k0$ observed reflection peaks,

$$d_{100}(\text{calcd}) = \frac{1}{N_{h00}} \left[\sum_{h00} d_{h00}(\text{obs}) h \right] \quad (11)$$

(where N_{h00} is the number of $h00$ observed reflections), and use this re-evaluated value of d_{100} in equation (12) for re-evaluating d_{010} :

$$d_{010}(\text{calcd}) = \frac{1}{N_{hk0}} \left[\sum_{hk0} k / \left(\frac{1}{d_{hk0}^2(\text{obs})} - \frac{h^2}{d_{100}^2(\text{calcd})} \right)^{1/2} \right] \quad (12)$$

(where N_{hk0} is the number of $hk0$ observed reflections). In the opposite case (when $N_{0k0} > N_{h00}$), the re-evaluation of d_{010} should be performed first. This can be achieved by rewriting equation (11) for d_{010} . Then, d_{100} will be obtained through the appropriate transcription of equation (12).

The Col_l refinement procedure can be performed through an analogous methodology. Since in this particular rectangular lattice d_{100} is equal to d_{010} , only the re-evaluation of the first interplanar distance value is necessary. This can be achieved *via*

$$d_{100}(\text{calcd}) = \frac{1}{N_{hk0}} \left[\sum_{hk0} d_{hk0}(\text{obs}) (h^2 + k^2)^{1/2} \right], \quad (13)$$

where N_{hk0} is the number of $hk0$ observed reflections. Finally, the Col_o refinement procedure requires the redetermination of the two first interplanar distance values d_{100} and d_{010} as well as the re-evaluation of the γ angle, which can be achieved by the following equations:

$$d_{100}(\text{calcd}) = \frac{1}{N_{h00}} \left(\sum_{h00} d_{h00}(\text{obs}) h \right), \quad (14)$$

where N_{h00} is the number of $h00$ observed reflections,

$$d_{010}(\text{calcd}) = \frac{1}{N_{0k0}} \left(\sum_{0k0} d_{0k0}(\text{obs}) k \right), \quad (15)$$

where N_{0k0} is the number of $0k0$ observed reflections, and

$$\cos \gamma(\text{calcd}) = \frac{1}{N_{hk0}} \left[\sum_{hk0} \frac{1}{2hk} \left(\frac{h^2 d_{010}(\text{calcd})}{d_{100}(\text{calcd})} + \frac{k^2 d_{100}(\text{calcd})}{d_{010}(\text{calcd})} - \frac{d_{100}(\text{calcd}) d_{010}(\text{calcd})}{d_{hk0}^2(\text{obs})} \right) \right], \quad (16)$$

where N_{hk0} is the number of $hk0$ observed reflections.

2.6. Number of molecules in discoids

Once the indexing of a PXRD pattern of a columnar liquid crystal has been performed, the number of molecules within the discoid at the origin of the columnar stacking can be determined, but only for ordered phases (*i.e.* when the $h_0 = d_{001}$ reflection peak is present). The number of molecules per unit cell (or cross section) (z) can be estimated according to (Lehmann *et al.*, 2006)

$$z = \rho N_A S h_0 / M, \quad (17)$$

where ρ is the density of the liquid crystal phase, N_A is Avogadro's constant, S is the columnar cross-section area, h_0 is the height of the columnar slice and M is the molecular weight of the constitutive molecule. S can be easily calculated from the cell parameters, keeping in mind that its expression depends on the geometry of the cell (see Table 1). The liquid crystal density can be estimated unless measured experimentally. Density values ranging from 0.9 g cm⁻³ up to 1.2 g cm⁻³ have been reported depending on the nature of the studied liquid crystals (full organic molecules, metallomesogens, neutral or ionic mesogens) (Gunyakov *et al.*, 2003; Kaller *et al.*, 2009, 2010; Ionescu *et al.*, 2012). The number of discoids present in the unit cell (Z_{disc}) is characteristic of the lattice geometry and the proposed model (see Table 1). Consequently, the number of molecules per discoid (N) is easily accessible by dividing the number of molecules in the cross section (z) by the corresponding Z_{disc} value. Therefore, a hypothesis on how mesogen molecules are eventually organized to form the discoidal shape can be formulated. This finding can be further supported by experimental data when intradiscoidal stacking gives rise to sufficiently intense reflections in the wide-angle region of the PXRD pattern (see Fig. 2). In the absence of such information, only theoretical modelling can shed light on the discoidal molecular assembly. However, it has to be mentioned that this calculation is based on the initial hypothesis that columns are organized in the mesophase with a straight vertical stacking order. In reality the intracolumnar stacking distance h might be higher or lower than h_0 . This is the case for tilted ($h > h_0$) and undulating ($h < h_0$) columnar organizations (Weber *et al.*, 1991; Donnio *et al.*, 1997). Neither case will be considered by *LCDiXRay* in its current version, but they will be considered in future upgrades.

3. Software description and examples

3.1. Algorithm and software implementation

A user-friendly program has been implemented in a Java object-oriented framework in order to identify correctly the mesophase *via* indexing of PXRD patterns and, as a conse-

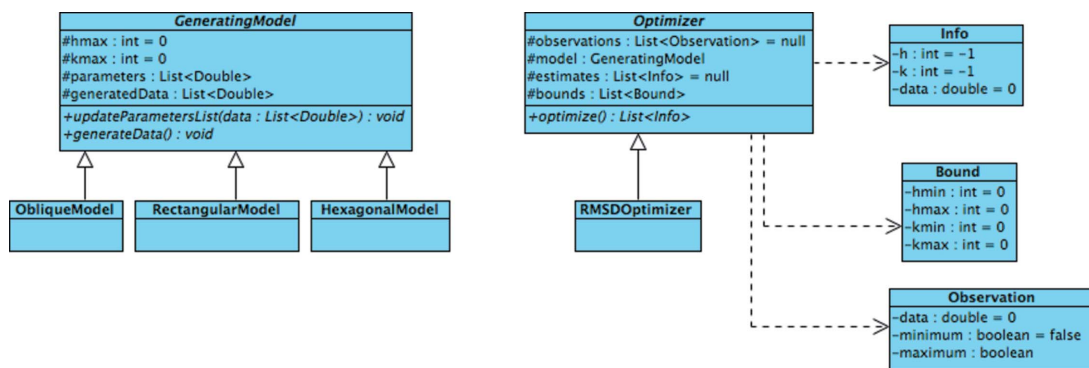


Figure 3
Class diagram of the *LCDiXRay* algorithm.

quence, determine the optimal parameters best fitting the observed data. It is worth underlining the advances in terms of computational speed of the proposed approach. The framework has been designed on the basis of the previously described indexing procedures for Col_h , Col_r , Col_t and Col_o mesophases.

The core idea is to rewrite the experimental data d_i as a function of the peak indices h_i , k_i and unknown parameters $\{p_k\}_{k=1}^n$ for all types of mesophase according to the following equation:

$$d_i = f(h_i, k_i, p_1, \dots, p_n). \quad (18)$$

For all the discussed mesophase types, a relative interface has been initialized with appropriate methods as shown in the class diagram reported in Fig. 3.

The mathematical equations of the interplanar distances [equations (2)–(4)] can be described in the form of equation (18) with $\{p_k\}_{k=1}^n$ representing the unknown structural parameters of the hypothesized mesophase. Given an n -length user-selected input data set $\{d_k\}_{k=1}^n$, coupled with n different indices (h_i, k_i) , the related n parameters are computed by solving the system formed by the n equations derived from equation (18). Once such parameters are obtained, an estimate d_{gen} of the entire experimental data set is generated by varying the indices h and k in an appropriate user-selected discrete grid. An optimization search is performed with the

indexing couples (h_i, k_i) as control parameters, by considering a root-mean-square difference (RMSD) optimization process:

$$RMSD = \left[\sum_{i=1}^{n_{obs}} (d_{obs} - d_{gen})^2 \right]^{1/2}. \quad (19)$$

The output of the above procedure represents the set of optimal parameters providing the minimum RMSD index value within the range of user-selected discrete indices, according to the chosen generation model.

The generation model, *i.e.* hexagonal, rectangular or oblique, and the data set extracted from the experimental PXRD pattern are needed as initial input. The Java program is characterized by dynamic panels that are updated according to the chosen generation model and provides a test on the consistency of the data set for the indexing problem. The class diagram of the designed user interface is depicted in Fig. 4.

The ‘InteractiveTableModel’ provides useful tools to choose an appropriate number of observed peaks representing the initial hypothesis for the indexing algorithm from which all the lattice parameter(s) will be determined. It is also possible to select the Miller index range defining the admissible indexing values. A similar range definition is required in the generation process of the estimated data set. To this end, two Miller indices (h_{max} and k_{max}) represent the maximum admissible values to generate all the observed diffraction peaks. An appropriate choice of parameters h_{max} and k_{max} is required to avoid a set of d_{hk0} indexing that does not have any realistic significance but which could mathematically result in a lower RMSD index.

Finally, once a convergent result has been obtained which suits the user’s expectations, a pop-up menu allows them, as a first option, to proceed to the refinement of the indexing, following the methodologies previously described. A second option allowing the determination of the number of molecules within the discoid is also accessible only for ordered mesophases.

Ultimately, all the generated data, the indexing set and the optimal parameters can be exported for further manipulations.

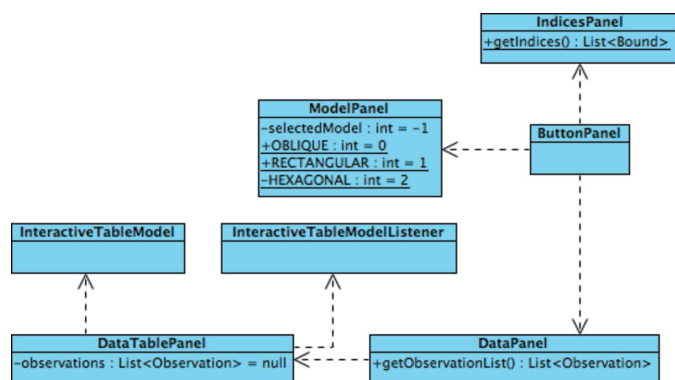


Figure 4
Class diagram of the user interface developed for *LCDiXRay*.

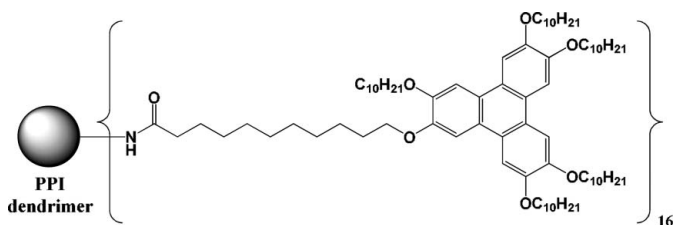


Figure 5
Discotic (I), an example of a Col_h mesophase (McKenna *et al.*, 2005).

Peak	d_{obs} (Å) ¹	d_{calc} (Å)	Miller indices hkl
d_1	58.1	57.8	100
d_2	33.4	33.4	110
d_3	28.9	28.9	200
d_4	21.7	21.8	210
d_5	19.1	19.3	300
d_6	16.0	16.0	310
d_7	14.4	14.4	400
d_8	13.2	13.3	320
d_9	12.7	12.6	410
d_{10}	4.5	-	h_{CH}
d_{11}	3.55	-	h_0
$a_h = 66.7 \text{ \AA}$			

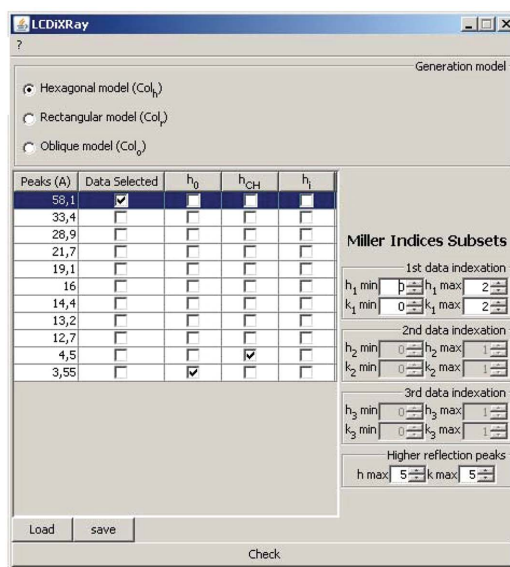


Figure 6
 d spacings and lattice parameter for the ordered columnar hexagonal mesophase Col_{h_0} of discotic (I), and the corresponding *LCDiXRay* program window.

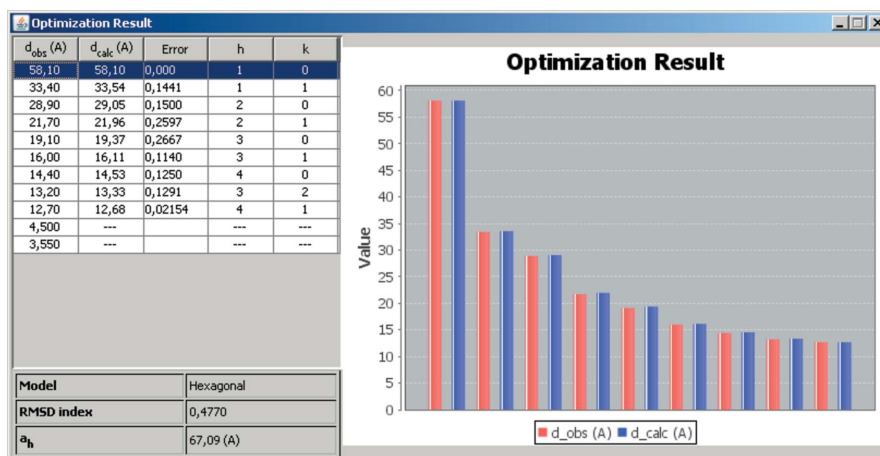


Figure 7
Obtained *LCDiXRay* result.

3.2. Practical examples

3.2.1. Ordered hexagonal columnar mesophase. Although the indexing of a Col_h mesophase is rather straightforward to perform because of the characteristic ratios between the observed peaks of a PXRd pattern (see §2.1), the following example of a Col_{h_0} discotic mesophase exhibited by discotic

(I) (see Fig. 5) (McKenna *et al.*, 2005), a poly(propylene imine) dendrimer based on a triphenylene, is a perfect example to illustrate at first glance the performance of the *LCDiXRay* program. The experimental and calculated literature data for (I) are presented in Fig. 6, together with the initial window frame relative to the loaded data.

The hexagonal model has been selected on the *LCDiXRay* program window, as well as the first observed peak ($d_1 = 58.1 \text{ \AA}$), which will be taken into account to determine the lattice parameter. On the far right of the program window, only the first Miller index subset is active, corresponding to the user-selected discrete grid of indices allowed for the selected initial peak. Having chosen as a first subset the values 0 and 2 for h_1 and k_1 minimum and maximum, respectively, the only possible values to be considered for d_1 are $d_{hk0} = d_{100}, d_{200}, d_{110}, d_{210}$ and d_{220} . Finally, on the bottom right of the window, the maximum values of h and k Miller indices that will be considered to index all observed peaks (d_2 – d_9) have both been fixed equal to 5. Note that the 11th observed peak $d_{11} = 3.55 \text{ \AA}$ has been assigned as h_0 and the tenth peak $d_{10} = 4.5 \text{ \AA}$ has been assigned as h_{CH} ; both values will therefore be removed from the fitting procedure. The active window obtained after a validation check is presented in Fig. 7, clearly showing the expected fitting for a hexagonal lattice with an RMSD index of 0.4770 for a lattice parameter of $a_h = 67.09 \text{ \AA}$. To reproduce exactly the literature data reported in Fig. 6 (McKenna *et al.*, 2005), the initial selected peak (from which all calculations are performed) must be $d_3 = 28.9 \text{ \AA}$ (see supplementary information¹), the initial choice made by the authors. In these conditions, an RMSD index of 0.3933 and a lattice parameter $a_h = 66.74 \text{ \AA}$ are obtained.

An active pop-up window in *LCDiXRay* allows the user to proceed to the data refinement to reduce eventually the RMSD between experimental and

calculated interplanar distances, according to the method previously described. The refined data reported in Fig. 8 and obtained from the optimization results based on the selected

¹ Supporting information for this article is available from the IUCr electronic archives (Reference: NB5093).

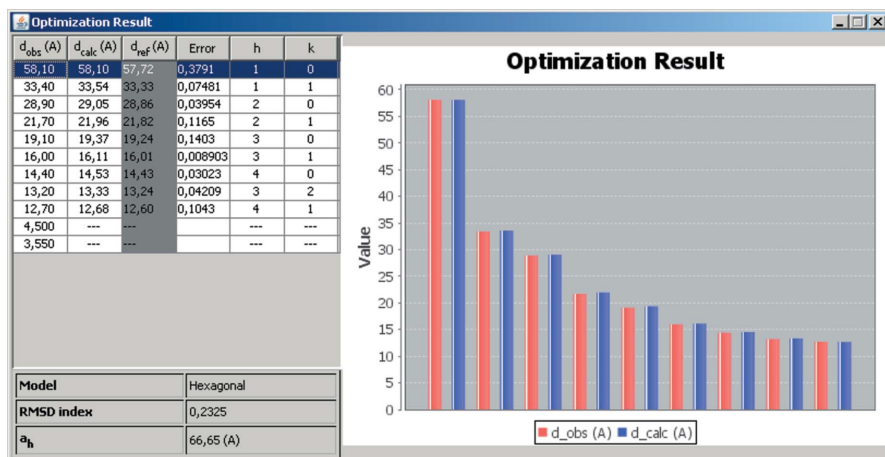


Figure 8
LCDiXRay results obtained after refinement.

observed peak at 58.1 Å show the lowering of the RMSD index to 0.2324 with a final lattice parameter $a_h = 66.65$ Å. Note that this RMSD index is even lower than that obtained reproducing the literature indexing (i.e. considering $d_3 = 28.9$ Å as initial selected peak).

Through this example, we can clearly see the genuine performance of LCDiXRay, allowing in a few clicks the generation of the optimized indexing despite the initial assumption made.

3.2.2. Ordered rectangular columnar mesophase with determination of the number of molecules within a discoid. A relevant example of the indexing of a Col_r mesophase is represented by the discotic mesophase exhibited by the

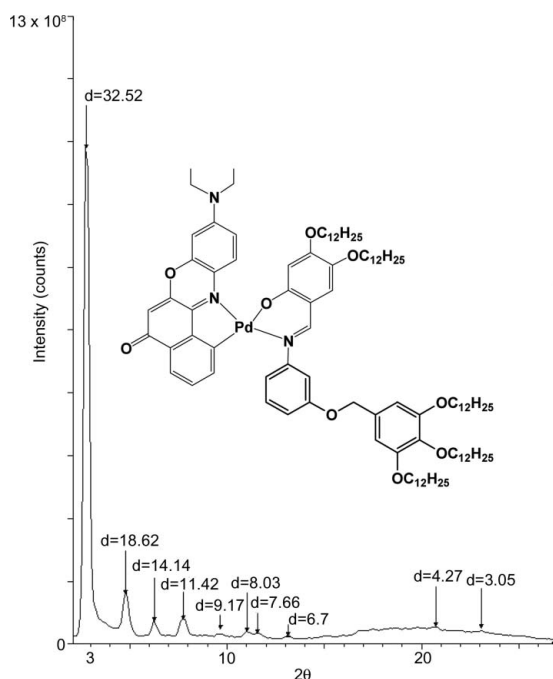
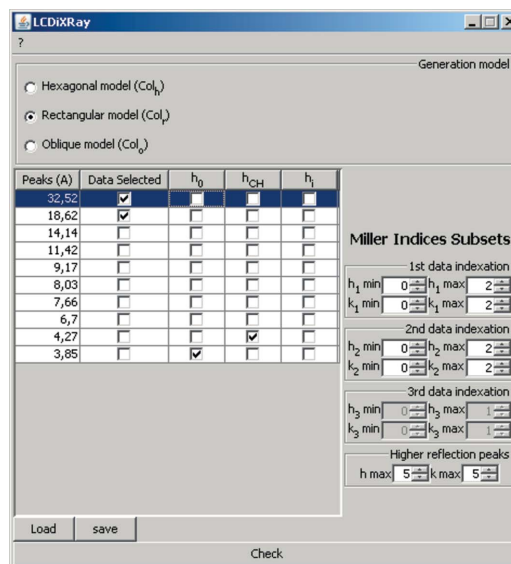


Figure 9
Discotic (II), an example of a Col_r mesophase, and its PXRd pattern recorded at 398 K after cooling from 433 K (Ionescu *et al.*, 2012).

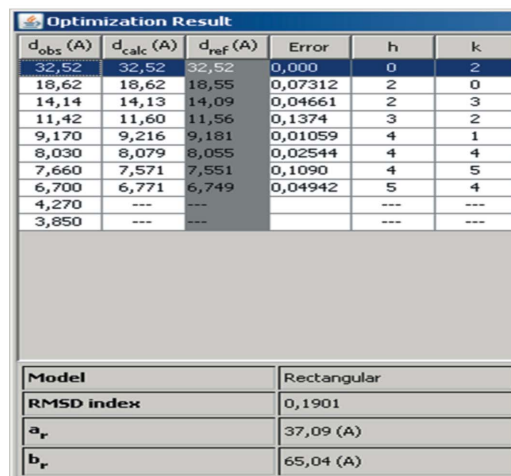
cyclopalladated photoconductive Nile red complex (II) (Fig. 9) (Ionescu *et al.*, 2012).

The active LCDiXRay window of the loaded interplanar distances observed on the PXRd pattern of discotic (II) with its initial assignment, together with the LCDiXRay result window obtained after checking the hypothesis of a Col_r model and refinement of the obtained preliminary results, are shown in Fig. 10.

Starting from the loaded data (active window of LCDiXRay; Fig. 10a) a two-click procedure (check and refinement; supplementary Figs. S2 and S3) allows the visualization of the most probable indexing of the mesophase of (II) through a Col_r model (Fig. 10b). We obtain a final RMSD value of 0.1901 with lattice parameters $a_r = 37.09$ Å and $b_r = 65.04$ Å. In



(a)

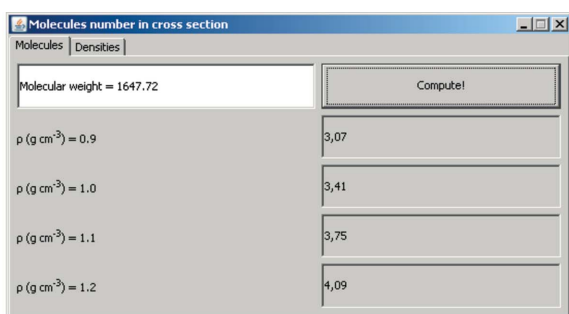


(b)

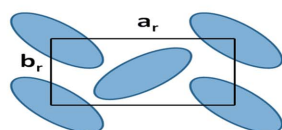
Figure 10
LCDiXRay results obtained for discotic (II) in a Col_r model.

this case, the first two observed peaks were initially chosen to perform all calculations, with a selected discrete grid of Miller indices ranging from 0 to 2 ($h_{\min} = k_{\min} = 0$; $h_{\max} = k_{\max} = 2$, with $i = 1$ or 2).

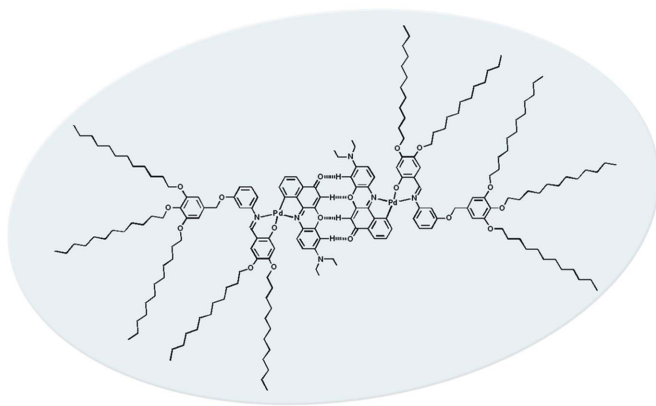
A second activated window allows the determination of the number of molecules within the cross-section area of the unit cell, as illustrated in Fig. 11(a). Following equation (2), the number of molecules present within the cross section has been determined for four different standard density values. As expected for metallomesogens, a density of 1.2 g cm^{-3} can reasonably be attributed for discotic (II), resulting in four molecules being present in the cross section. According to the obtained indexing together with the extinction rules (see Table 1), the space group of the mesophase for (II) can be deduced as $p2gg$. Unequivocally, since in the $p2gg$ space group two discoids are present in the unit cell ($Z_{\text{disc}} = 2$; Fig. 11b), each disc contains two molecules, forming a dimer-like discoid. Theoretical calculations have been performed confirming the existence of a hydrogen-bond network established between two side-by-side molecules placed in a head-to-tail arrangement as illustrated in Fig. 11(c) (Ionescu *et al.*, 2012).



(a)



(b)



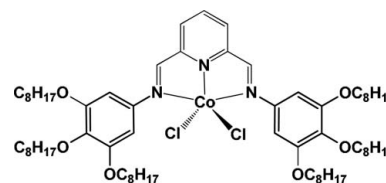
(c)

Figure 11

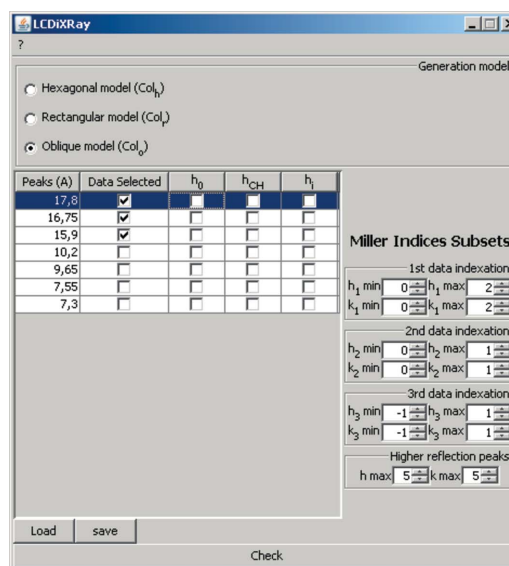
(a) *LCDiXRay* active window, (b) representation of a cross-section area of a $p2gg$ lattice (c) and schematic representation of the dimer of (II) generating a discoid.

3.2.3. Disordered oblique columnar mesophase. Finally, to illustrate the performance and the swiftness of the *LCDiXRay* program, the identification of a columnar oblique mesophase is presented through the indexing of the PXR D pattern recorded at 393 K for the cobalt complex (III) (see Fig. 12) (Morale *et al.*, 2003).

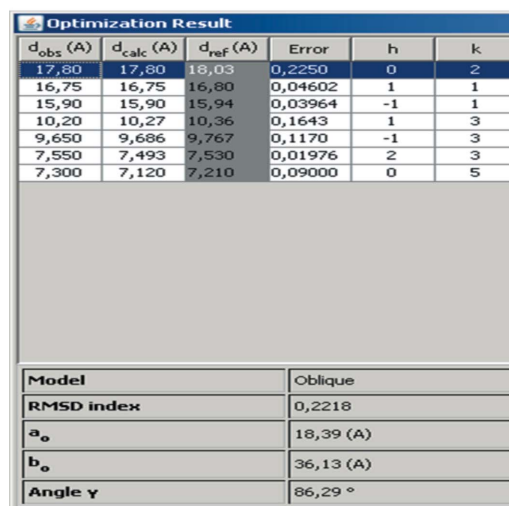
As shown in Fig. 13(a) for the Col_o model, all subsets of the *LCDiXRay* program window are now activated, since three interplanar distances have to be initially selected to index as a


Figure 12

Discotic (III), an example of a Col_o mesophase (Morale *et al.*, 2003).



(a)



(b)

Figure 13

LCDiXRay results obtained for discotic (III) in a Col_o model.

Col_o lattice. The literature-reported interplanar distances have been loaded and, again, in only one validation click, the results window allows us to check the feasibility of the Col_o hypothesis. The results window (Fig. 13b) gives the indexing with the smallest RMSD between experimental and calculated distances, based as always on the user-selected choice of the initial Miller indices. The obtained results are in agreement with reported literature data.

Note that in this example the refinement of the data performed following the previously described procedure will lead to a slight increase of the RMSD value, which varies from 0.2038 (unrefined) to 0.2218 (refined) (supplementary Figs. S4 and S5). This is due to the small number of observed reflection peaks on which obviously all the calculations are based. In particular, the lack of *0k0* reflection peaks means that the *d*₀₁₀ reflection value has to be fixed, excluding it from the refinement. Since for Col_o mesophases three initial peaks are required, the refinement tool can only achieve realistic results when a large number of reflection peaks are observed, which is unfortunately rarely encountered for this type of mesophase.

3.3. Experimental errors

LCDiXRay performs the refinement procedure from the loaded interplanar distances values, although the scattering angles 2θ are the experimental data collected over an X-ray powder diffraction analysis. The 2θ experimental error is highly dependent on the experimental technique used (reflection *versus* transmission). Furthermore, the interplanar distance accuracy is intrinsically generally much lower for large *d* values than for low *d* values. Not surprisingly, throughout the literature on PXRd of liquid crystal mesophases, data accuracy is most of the time left undiscussed and experimental data are reported in *d* values in ångström with one (in most cases) or at most two digits. In some cases, to take into account such error in the accurate determination of distances, several indexings of possible Miller indices are proposed. For all these reasons, the current version of *LCDiXRay* will not take into account this unpredictable experimental error. Consequently, the RMSD index given by *LCDiXRay* is mostly indicative and only relevant for comparisons, and the accuracy of the lattice constant values obtained through the program must be critically evaluated by the user. Similarly, in its current version only one set of data is proposed by the software, which corresponds to the lowest RMSD value obtained from the loaded values and initial restrictions. The proposal of several solutions, with restricted deviations reflecting the experimental errors obtained during the recording of the PXRd pattern, will be implemented in the near future.

4. Conclusions

LCDiXRay is a user-friendly program for powder diffraction indexing of columnar liquid crystals. The main objective of this powerful tool is to accelerate the determination of the exact nature of the mesophase presented by columnar LCs.

Furthermore, the program contains all the mathematical expressions required for data refinement and determination of structural parameters of the identified mesophases (unit-cell geometry and dimensions, cross-area section, number of molecules within the discoid for ordered phases). The determination of columnar mesophases, in particular Col_r and Col_o, is often performed manually; *LCDiXRay* is able in a few minutes to perform all the time-consuming operations and provide the most likely indexing of a recorded PXRd pattern. Further implementations of *LCDiXRay* are planned in due course and will concern also the determination of the most likely space group for Col_r mesophases on the basis of the extinction rules characterizing them, as well as the possibility of performing a refinement of Col_r data as a Col_t mesophase when the cell parameters are compatible (*a_r* \simeq *b_r*). Finally, it is expected that a similar procedure will be introduced for the indexing of calamitic mesophases, allowing the inclusion in *LCDiXRay* of lamellar columnar and non-classical mesophases, such as plastic columnar phases or the three-dimensionally highly ordered mesophases (H phase).

The *LCDiXRay* program is freely available from the authors on request. We would like to suggest that users send feedback for future improvements. A request form is available in the supporting information.

This work was supported by the European Community's Seventh Framework Programme (FP7 2007–2013), through the MATERIA project (PONa3_00370).

References

- Camerel, F., Donnio, B., Bourgoigne, C., Schmutz, M., Guillon, D., Davidson, P. & Ziessel, R. (2006). *Chem. Eur. J.* **16**, 4261–4274.
- Chandrasekhar, S., Krishna Presad, S., Shankar Rao, D. S. & Balagurusamy, V. S. K. (2002). *Proc. Indian Natl Sci. Acad.* **68A**, 175–191.
- Chandrasekhar, S., Sadashiva, B. K. & Suresh, K. A. (1977). *Pramana*, **9**, 471–480.
- Chen, B., Baumeister, U., Pelzl, G., Das, M. K., Zeng, X., Ungar, G. & Tschierske, C. (2005). *J. Am. Chem. Soc.* **127**, 16578–16591.
- Choi, J., Han, J., Ryu, M. & Cho, B. (2011). *Bull. Korean Chem. Soc.* **32**, 781–782.
- Donnio, B., Heinrich, B., Gulik-Grzywicki, Th., Delacroix, H., Guillon, D. & Bruce, D. W. (1997). *Chem. Mater.* **9**, 2951–2965.
- Gehring, L., Bourgoigne, C., Guillon, D. & Donnio, B. (2005). *J. Mater. Chem.* **15**, 1696–1703.
- Grolik, J., Dudek, L., Eilmes, J., Eilmes, A., Górecki, M., Frelek, J., Heinrich, B. & Donnio, B. (2012). *Tetrahedron*, **68**, 3875–3884.
- Guillon, D., Skoulios, A. & Malthete, J. (1987). *Europhys. Lett.* **3**, 67–72.
- Gunyakov, V. A., Shestakov, N. P. & Shibli, S. M. (2003). *Liq. Cryst.* **30**, 871–875.
- Hesse, H. C., Weickert, J., Al-Hussein, M., Dössel, L., Feng, X., Müllen, K. & Schmidt-Mende, L. (2010). *Sol. Energ. Mater. Sol. Cells*, **94**, 560–567.
- Ionescu, A., Godbert, N., Crispini, A., Termine, R., Golemme, A. & Ghedini, M. (2012). *J. Mater. Chem.* **22**, 23617–23626.
- Kaafarani, B. R. (2011). *Chem. Mater.* **23**, 378–396.
- Kaller, M., Deck, C., Meister, A., Hause, G., Baro, A. & Laschat, S. (2010). *Chem. Eur. J.* **16**, 6326–6337.

- Kaller, M., Tussetschlager, S., Fischer, P., Deck, C., Baro, A., Giesselmann, F. & Laschat, S. (2009). *Chem. Eur. J. Chem.* **15**, 9530–9542.
- Kato, T., Mizoshita, N. & Kishimoto, K. (2006). *Angew. Chem. Int. Ed.* **45**, 38–68.
- Kilian, D., Knawby, D., Athanassopoulou, M. A., Trzaska, S. T., Swager, T. M., Wrobel, S. & Haase, W. (2000). *Liq. Cryst.* **27**, 509–521.
- Komatsu, T., Ohta, K., Watanabe, T., Ikemoto, H., Fujimoto, T. & Yamamoto, I. (1994). *J. Mater. Chem.* **4**, 537–540.
- Kumar, S. (2006). *Chem. Soc. Rev.* **35**, 83–109.
- Laschat, S., Baro, A., Steinke, N., Giesselmann, F., Hägele, C., Scalia, G., Judele, R., Kapatsina, E., Sauer, S., Schreivogel, A. & Tosoni, M. (2007). *Angew. Chem. Int. Ed.* **46**, 4832–4887.
- Lehmann, M., Köhn, C., Meier, H., Renker, S. & Oehlhof, A. (2006). *J. Mater. Chem.* **16**, 441–451.
- Levelut, A. M. (1983). *J. Chim. Phys.* **80**, 149–161.
- Li, J., He, Z., Zhao, H., Gopee, H., Kong, X., Xu, M., An, X., Jing, X. & Cammidge, A. N. (2010). *Pure Appl. Chem.* **82**, 1993–2003.
- Maringa, N., Lenoble, J., Donnio, B., Guillon, D. & Deschenaux, R. (2008). *J. Mater. Chem.* **18**, 1524–1534.
- McKenna, M. D., Barberá, J., Marcos, M. & Serrano, J. L. (2005). *J. Am. Chem. Soc.* **127**, 619–625.
- Morale, F., Date, R. W., Guillon, D., Bruce, D. W., Finn, R. L., Wilson, C., Blake, A. J., Schröder, M. & Donnio, B. (2003). *Chem. Eur. J.* **9**, 2484–2501.
- Ohta, K., Watanabe, T., Hasebe, H., Morizumi, Y., Fujimoto, T., Yamamoto, I., Lelièvre, D. & Simon, J. (1991). *Mol. Cryst. Liq. Cryst.* **196**, 13–26.
- Pucci, D., Barberio, G., Bellusci, A., Crispini, A., La Deda, M., Ghedini, M. & Szerb, E. I. (2005). *Eur. J. Inorg. Chem.* **12**, 2457–2463.
- Pucci, D., Crispini, A., Ghedini, M., Szerb, E. I. & La Deda, M. (2011). *Dalton Trans.* **40**, 4614–4622.
- Reddy, R. A., Raghunathan, V. A. & Sadashiva, B. K. (2005). *Chem. Mater.* **17**, 274–283.
- Schmidt-Mende, L., Fechtenkötter, A., Müllen, K., Friend, R. & MacKenzie, J. (2002). *Physica E*, **14**, 263–267.
- Seo, J., Kim, S., Gihm, S. H., Park, C. R. & Park, S. Y. (2007). *J. Mater. Chem.* **17**, 5052–5057.
- Sergeyev, S., Pisula, W. & Geerts, Y. H. (2007). *Chem. Soc. Rev.* **36**, 1902–1929.
- Shimizu, Y., Oikawa, K., Nakayama, K. & Guillon, D. (2007). *J. Mater. Chem.* **17**, 4223–4229.
- Shimogaki, T., Dei, S., Ohta, K. & Matsumoto, A. (2011). *J. Mater. Chem.* **21**, 10730–10737.
- Trzaska, S. T., Zheng, H. & Swager, T. M. (1999). *Chem. Mater.* **11**, 130–134.
- Tschierske, C. (2007). *Chem. Soc. Rev.* **36**, 1930–1970.
- Venkatesan, K., Kouwer, P. H. J., Yagi, S., Müller, P. & Swager, T. M. (2008). *J. Mater. Chem.* **18**, 400–407.
- Weber, P., Guillon, D. & Skoulios, A. (1991). *Liq. Cryst.* **9**, 369–382.
- Wuckert, E., Hägele, C., Giesselmann, F., Baro, A. & Laschat, S. (2009). *Beilstein J. Org. Chem.* **5**, 57.
- Zelcer, A., Donnio, B., Bourgogne, C., Cukiernik, F. D. & Guillon, D. (2007). *Chem. Mater.* **19**, 1992–2006.
- Zheng, Q., Fang, G., Sun, N., Qin, P., Fan, X., Cheng, F., Yuan, L. & Zhao, X. (2011). *Sol. Energ. Mater. Sol. Cells*, **95**, 2200–2205.